

Supporting information

Clarifying the dehydrogenation pathway of catalysed $\text{Li}_4(\text{NH}_2)_3\text{BH}_4$ -LiH composite

Guillermina Amica^a, Ewa C. E. Rönnebro^b, Pierre ArneodoLarochette^a, Fabiana C. Gennari^a*

- a. Consejo Nacional de Investigaciones Científicas y Técnicas, CONICET - Instituto Balseiro (UNCuyo and CNEA). Centro Atómico Bariloche (CNEA), R8402AGP, S. C. de Bariloche, Río Negro, Argentina
- b. Pacific Northwest National Laboratory, 902 Battelle Boulevard, Richland, WA 99352, USA

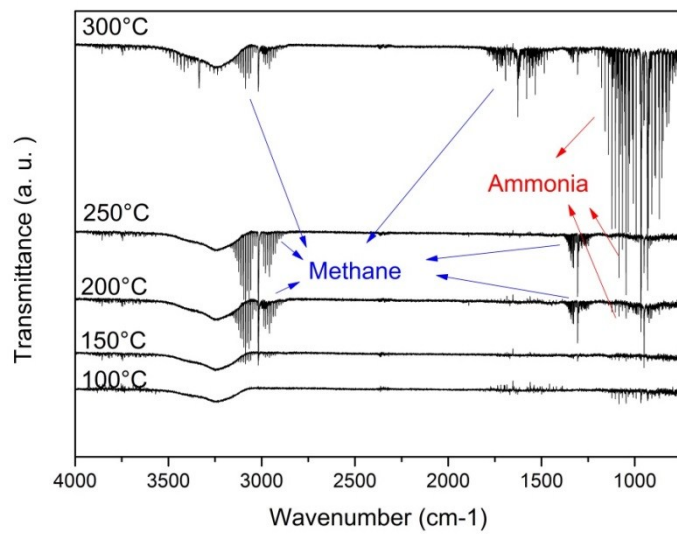


Figure S1: FTIR gas spectra for the $\text{Li}_4(\text{NH}_2)_3\text{BH}_4$ - LiH composite.

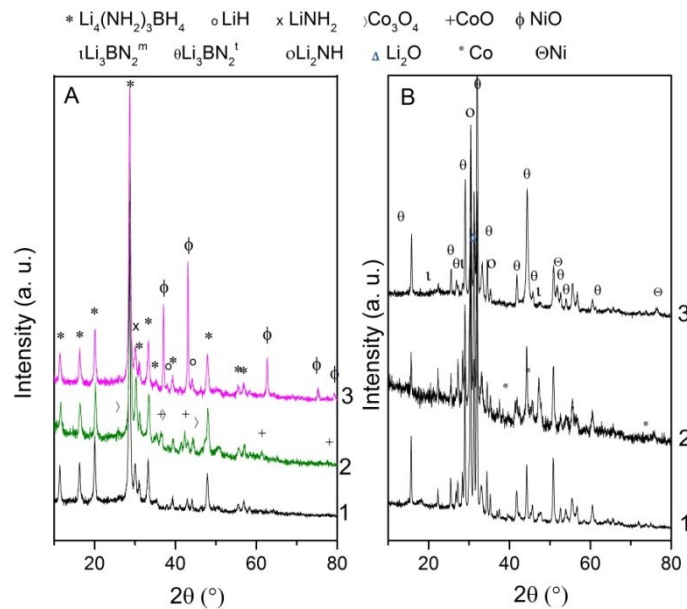


Figure S2: PXRD of samples $\text{Li}_4(\text{NH}_2)_3\text{BH}_4$ - LiH (1), $\text{Li}_4(\text{NH}_2)_3\text{BH}_4$ - LiH - Co_2O_3 (2) and $\text{Li}_4(\text{NH}_2)_3\text{BH}_4$ - LiH - NiO (3) after mechanical milling and dehydrogenation.

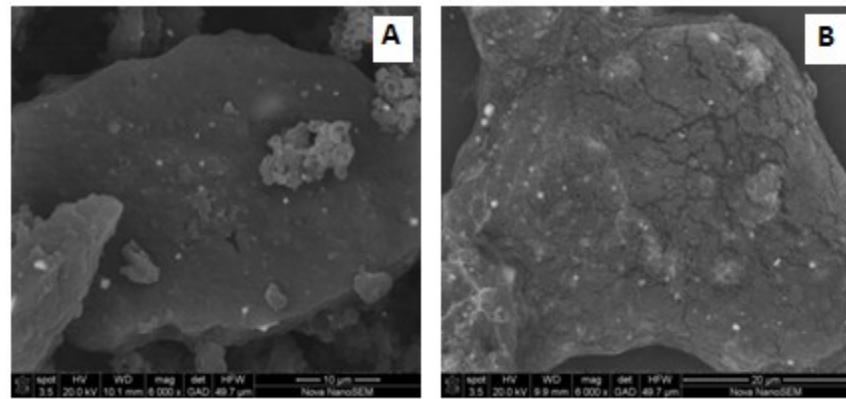


Figure S3: SEM images of ball milled samples $\text{Li}_4(\text{NH}_2)_3\text{BH}_4$ - LiH - Co_2O_3 (A) and $\text{Li}_4(\text{NH}_2)_3\text{BH}_4$ - LiH - NiO (B).

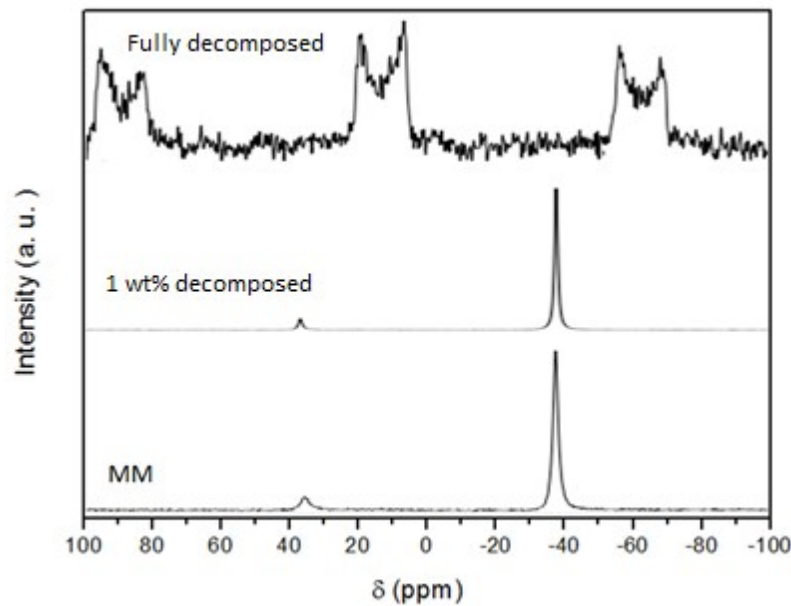


Figure S4: NMR spectra of the $\text{Li}_4(\text{NH}_2)_3\text{BH}_4$ - LiH - NiO sample at different stages of dehydrogenation.

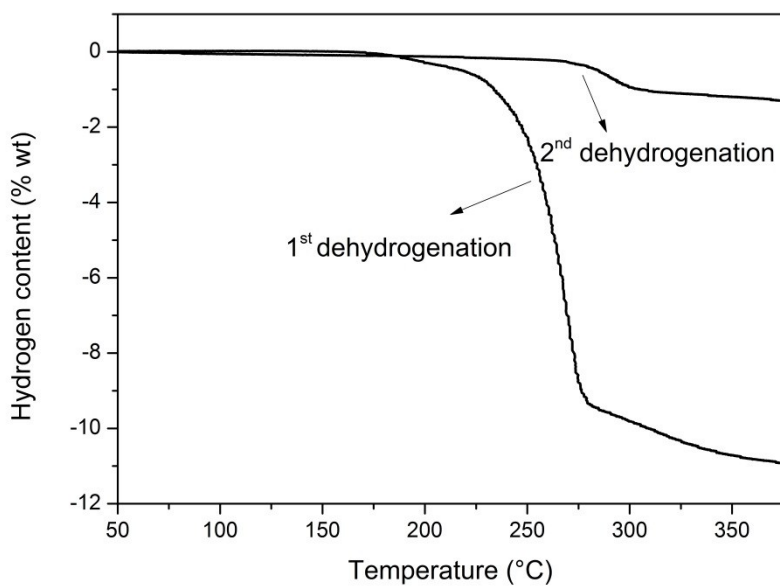


Figure S5: First and second dehydrogenation curve for the $\text{Li}_4(\text{NH}_2)_3\text{BH}_4$ - LiH - NiO sample.

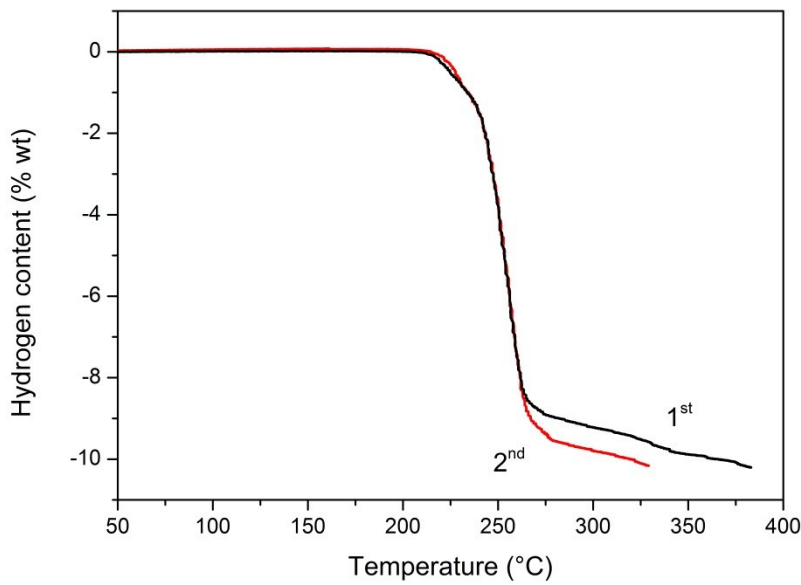


Figure S6: Comparison between two dehydrogenation runs after different times for sample $\text{Li}_4(\text{NH}_2)_3\text{BH}_4$ - NiO .

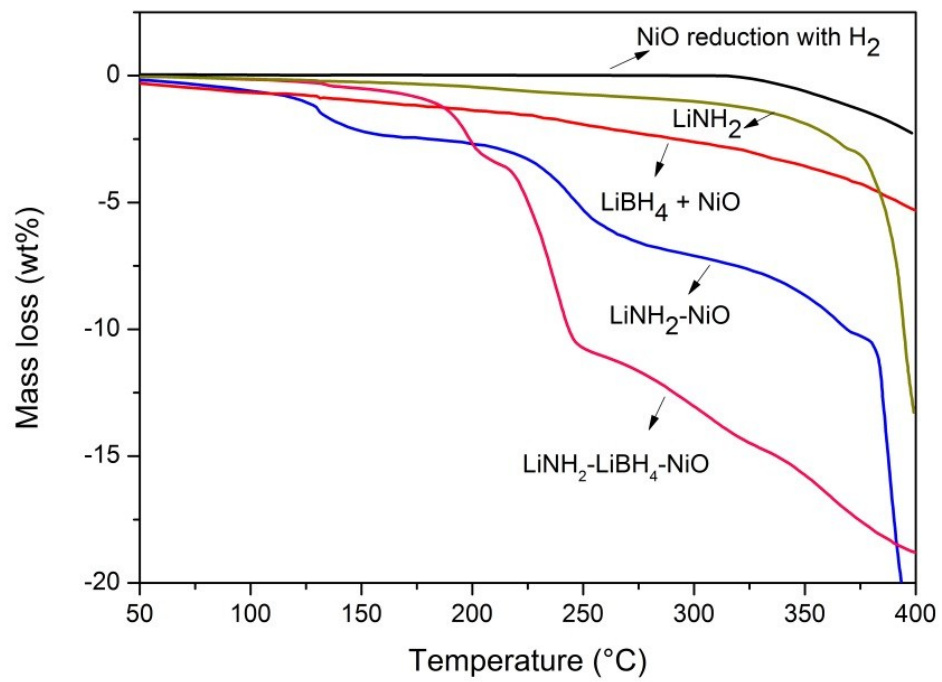


Figure S7: Additional thermogravimetric (TG) measurements.